Inorganic Chemistry

Article

pubs.acs.org/IC

When the Tolman Electronic Parameter Fails: A Comparative DFT and Charge Displacement Study of $[(L)Ni(CO)_3]^{0/-}$ and $[(L)Au(CO)]^{0/+}$

Gianluca Ciancaleoni,*[,†] Nicola Scafuri,[‡,§] Giovanni Bistoni,[†,‡] Alceo Macchioni,[‡] Francesco Tarantelli,[†,‡] Daniele Zuccaccia,[∥] and Leonardo Belpassi*[,†]

[†]Istituto di Scienze e Tecnologie Molecolari del CNR (CNR-ISTM), c/o Dipartimento di Chimica, Biologia e Biotecnologie, Università degli Studi di Perugia, I-06123, Perugia, Italy

[‡]Dipartimento di Chimica, Biologia e Biotecnologie, Università degli Studi di Perugia, Via Elce di Sotto 8, I-06123, Perugia, Italy

[∥]Dipartimento di Chimica, Fisica e Ambiente, Università di Udine, Via Cotonificio 108, I-33100 Udine, Italy

Supporting Information

ABSTRACT: In this study we have examined 42 $[(L)M(CO)_n]^{\pm/0}$ complexes (M = Ni and Au), including neutral ligands, such as phosphines and carbenes, and anionic ones. For each complex, the carbonyl stretching frequency (ν_{CO}) and the amount of charge donated from the ligand to the metal (CT) have been computed on the basis of DFT calculations. For nickel complexes, the two observables nicely correlate with each other, as expected from the theory underlying the Tolman electronic parameter. On the contrary, for gold complexes a more complex pattern can be observed, with an apparent differentiation between phosphine ligands and carbon-based ones. Such differences have been explained analyzing the Au−L bond in terms of Dewar−Chatt−Duncanson bonding constituents (σ donation and π back-donation). Our analysis demonstrates that in linear gold(I) complexes, ν_{CO} depends only on the metal-to-ligand π back-donation.

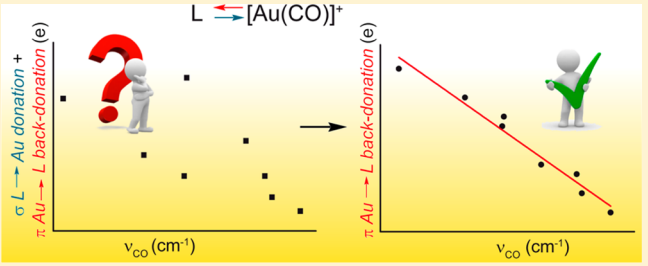

INTRODUCTION

The role of carbon monoxide (CO) in coordination chemistry has been crucial since 1890, when Ludwig Mond discovered the first nickel(0) carbonyl compound, $Ni(CO)_4$, and used this metal complex in an industrial process to produce pure nickel.[1] Today it is well-known that the CO molecule has a great affinity with many different metals, giving metal carbonyl complexes that play a key role in many catalytic processes (such as the industrially relevant Fischer−Tropsch process[2,3]), and allows chemists to explore in detail some fundamental catalytic steps, such as migratory insertion[4,5] and ligand substitution.[6] The possibility to characterize carbonyl complexes through a readily available analytical technique, IR spectroscopy,[7,8] represents a significant advantage. Furthermore—and this is a main motivation of the present work—the CO moiety is considered an excellent probe for the electronic properties of the metal fragment. Pioneering in this direction is Tolman's work on nickel(0) carbonyl complexes, from which the Tolman electronic parameter (TEP) emerged.[9] This is based on the IR frequency of the totally symmetric carbonyl stretching mode (ν_{CO}) of $[(L)Ni(CO)_3]$ in dichloromethane and is commonly considered a probe for the net donor power of a ligand, L.[10] This interpretation of the TEP is generally based on a simple model: if L donates electronic density to the metal, the latter transfers a certain "proportional" amount of electronic charge to the three CO groups as back-donation. Since the accepting CO orbitals have an antibonding π^* character (Scheme 1), the result is a weakening of the C−O bond that causes a red-shift of its stretching frequency (of note, a revisited version of the TEP, based on local CO stretching force constants rather than normal-mode frequencies, has been recently proposed[11]). Even if the original Tolman's work was about phosphine ligands, with time, several mono-*hapto* ligands were characterized through the measurement of their TEP. More recently, the possibility offered by the use of accurate density functional theory (DFT) methods[12] has permitted the study of different classes of ligands, even those difficult to handle or synthesize.

Scheme 1. Molecular orbitals involved in the M-CO coordinative bond

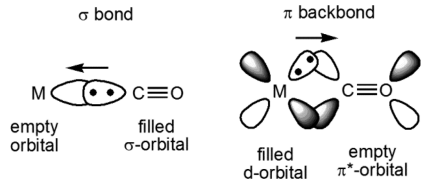

Many chemists tried to verify if the TEP is a good and general descriptor for the intrinsic electronic properties of a ligand (mainly within the phosphine class) and for its donor power, studying whether the trend in CO stretching frequency depended on the metal. Experimental and theoretical works on

Received: July 3, 2014
Published: August 28, 2014

   dx.doi.org/10.1021/ic501574e | *Inorg. Chem.* 2014, 53, 9907−9916

iridium,[13−15] rhodium,[16] and other metals[17,18] demonstrated that usually a good correlation between carbonyl stretching in $[(L)M(CO)_n]$ and TEP exists.[19−21] Such a good frequency/frequency correlation generally led to the deduction that the binding properties of ligands are almost independent of the metal, in agreement with the original Tolman's statement that the choice of transition metal carbonyl complex would be, in a sense, arbitrary.[19]

But the literature is not free from controversial and ambiguous results. For example, if the complexes $[(L)Ni(CO)_3]$ and *trans*-$[(L)_2RhCl(CO)]$ are considered, the respective IR data are best correlated with a quadratic function rather than a linear one,[22] while in the case of $[(L)Ni(CO)_3]$ and $[(L)Fe(CO)_4]$ practically no correlation is observed.[19] On the basis of a detailed comparative analysis examining different metal complexes, Gusev has recently questioned whether TEP values are useful for comparing ligands of different type, e.g., carbenes and phosphorus-based ligands.[23] Furthermore, according to K-edge X-ray absorption spectroscopy data on first- and second-generation Grubbs precatalysts, the net IMes → Ru donation (IMes = 1,3-bis(2,4,6-trimethylphenyl)-imidazol-2-ylidene) is smaller than the PCy_3 → Ru donation,[24] in contrast with the respective TEP values (2050 and 2056 for IMes and PCy_3, respectively) and with the accepted view of the bonding in these compounds.[21,25] Other inconsistencies are found in the case of $[(L)Cr(CO)_5]$. For this class of complexes, Hu and co-workers computed ν_{CO} and estimated L → Cr charge transfer[26] on the basis of electronic descriptors (such as electronegativity and hardness) of the partners L and $Cr(CO)_5$. According to their data, the correlation between ν_{CO} and the TEP is very satisfactory (r^2 = 0.9769), but, despite this, the correlation between ν_{CO} and the estimated donor ability of L is worse (r^2 = 0.9043), with a marked scattering of the data in the phosphines and carbenes region.[27] If the TEP was a good descriptor for the trend of bond properties with any metal, the charge transfer vs TEP correlation should have been as good as the one between ν_{CO} and TEP.

On the above grounds, it would seem that deducing from the TEP the nature of the ligand−metal bond may at times be unreliable. In general, understanding the electronic properties of a ligand is indeed a challenging task, but it appears essential for rational catalyst design. This is true, in particular, for gold-catalyzed processes, the focus of our attention here, where a detailed comprehension of ligand effects on the catalytic activation of a substrate is especially important.[28,29] Despite intense research activity in this field, there is still considerable debate regarding the nature of the Au−C bond, with particular reference to its "carbenoid" character.[30] In fact, it has been found that the amount of L−Au → substrate back-donation, which is strongly modulated by the ligand L, deeply influences the properties of the catalytic intermediates[31−33] and, in some cases, even the regioselectivity of the process.[34] Given these facts, it seems especially interesting to investigate gold carbonyl complexes $[(L)Au(CO)]^{+/0}$—which are linear and have no other interfering ligands—focusing on the ability of the carbonyl group to probe the electronic properties of the [(L)Au] fragment and on the relationship between the donor power of L and the Au−CO back-donation.

To the best of our knowledge, a systematic study of the relationship between the donor power of L and the IR frequency of CO in $[(L)Au(CO)]^{+/0}$ complexes, either experimental or theoretical, has never been done. Even if attention toward these systems is increasing, IR experimental data for $[(L)Au(CO)]^{+/0}$ complexes are available only for a handful of ligands.[35−45] Moreover, ligands with a small steric hindrance, such as halides and trifluoromethyl, allow two gold atoms to establish an aurophilic interaction[46,47] in the solid state[43] and in solution. In these cases, IR data could be influenced by the presence of small clusters, held together by Au−Au interactions.[42] Therefore, not all the literature values of ν_{CO} can be safely related to the donor power of L. For this reason, new experimental data, such as those reported by Dias et al., using phosphine and NHC (nitrogen heterocyclic carbene) ligands, would be highly relevant[41,42] (even if gold carbonyl complexes may present stability issues) and so are reliable theoretical calculations.

In this paper, using charge-displacement (CD) analysis[48−52] to reliably assess the donor ability of ligands, we report an extensive comparative DFT study on the relationship between the stretching frequency of CO, the donor power of L, and the extent of back-donation in [(L)Au], for both $[(L)Ni(CO)_3]^{0/-}$ and $[(L)Au(CO)]^{+/0}$ complexes.[48]

Scheme 2 shows a list of all the ligands (more than 20) considered here. Among them, phosphines with different

Scheme 2. List and abbreviations for the ligands considered in the present work

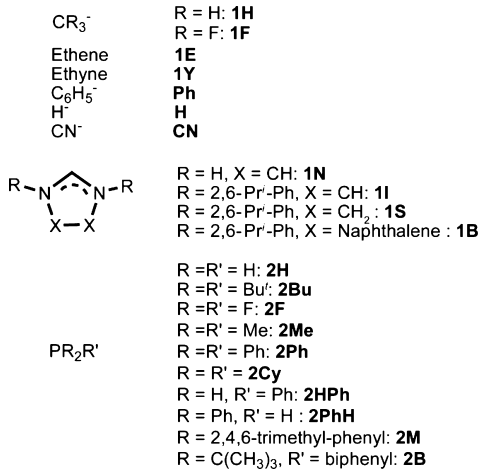

electronic and steric properties have been considered, such as the prototypical triphenylphosphine (**2Ph**), the sterically demanding trimesitylphosphine (**2M**), and the so-called JohnPhos (**2B**). The latter is part of the "Buchwald series",[53] and it exhibits quite peculiar steric properties, having a phenyl group protruding toward the metal and possibly interfering with the ligand in the *trans* position. Other ligands are bound to the metal through a sp^3 (such as the methyl, **1H**, and the fluorinated methyl, **1F**), sp^2 (phenyl, **Ph**, and carbenes, **1N**, **1I**, **1S** and **1B**), or *sp* (cyanide, **CN**) carbon atom or by a π system (ethene, **1E**, and ethyne, **1Y**). It is also evident that not all the ligands have the same charge.

For all the ligands shown in Scheme 2, the geometries of the complexes $[(L)Ni(CO)_3]^{0/-}$ (**L_Ni**, Table 1) and $[(L)Au(CO)]^{+/0}$ (**L_Au**, Table 2) have been optimized, and the harmonic frequencies have been computed by DFT methods. A quantitative evaluation of the net charge transfer (CT) between L and the metal fragments has been obtained by CD analysis as described later. This method gives a detailed spatial description of the electronic charge redistribution within the metal fragment induced by L-metal bond formation.

dx.doi.org/10.1021/ic501574e | Inorg. Chem. 2014, 53, 9907−9916

Table 1. Relevant Geometrical Parameters (distances in Å, angles in degrees), ν_{CO} (in cm^{-1}), and CT (in e) between L and Ni for L_Ni Complexes

L	C−O[a,b]	L−Ni−CO[a]	ν_{CO}[c]	CT
1H	1.174	101.7	1918	0.36
1F	1.166	106.0	1962	0.21
1E	1.154	107.5	2033	0.01
1Y	1.153	107.5	2035	0.01
Ph	1.169	103.9	1938	0.28
CN	1.165	106.5	1970	0.18
H	1.173	100.7	1927	0.29
1N	1.158	107.5	2005	0.07
1N′[d]	1.158	110.7	1999	0.06
1I	1.159	110.7	1995	0.03
1B	1.158	111.4	1995	0.03
1S	1.159	111.2	1996	0.03
2H	1.154	106.8	2031	0.02
2F	1.149	108.5	2058	−0.09
2Me	1.157	106.8	2011	0.09
2Bu	1.159	111.1	1999	0.11
2Ph	1.156	107.5	2014	0.08
2Cy	1.158	108.2	2000	0.11
2HPh	1.155	107.1	2024	0.05
2PhH	1.155	107.1	2018	0.06
2M	1.158	108.4	2004	0.10
2B	1.158	109.9	2001	0.07

[a]Average value. [b]Free CO: 1.137 Å. [c]Free CO: 2106 cm^{-1}. [d]L−Ni−CO angle constrained at 110.7.

Table 2. Relevant Geometrical Parameters (distances in Å, angles in degrees), ν_{CO} (in cm^{-1}), and CT (in e) between L and Au for L_Au Complexes

L	C−O[a]	L−Au−CO	ν_{CO}[b]	CT
1H	1.144	180.0	2064	0.36
1F	1.139	180.0	2104	0.30
1E	1.130	180.0	2169	0.23
1Y	1.130	180.0	2168	0.20
Ph	1.144	180.0	2061	0.37
CN	1.140	180.0	2100	0.29
H	1.141	180.0	2081	0.30
1N	1.133	179.6	2145	0.24
1I	1.136	180.0	2122	0.26
1S	1.136	180.0	2129	0.25
1B	1.138	180.0	2107	0.30
2H	1.130	180.0	2166	0.26
2F	1.128	180.0	2186	0.21
2Me	1.132	180.0	2145	0.33
2Bu	1.135	179.9	2123	0.40
2Ph	1.134	180.0	2132	0.40
2Cy	1.135	179.7	2125	0.43
2HPh	1.132	179.3	2153	0.31
2PhH	1.133	178.3	2141	0.35
2M	1.136	180.0	2114	0.43
2B	1.136	173.1	2115	0.35

[a]Free CO: 1.137 Å. [b]Free CO: 2106 cm^{-1}, $[AuCO]^+$: 2181 cm^{-1}.

We shall present and discuss the correlation between ν_{CO} and CT for the two metals in order to shed light on the effective information that can be extracted from the IR spectrum of these systems. Our analysis reveals deep-lying features of the metal coordination bond, whereby we show that in the case of $[(L)Ni(CO)_3]^{0/-}$ the TEP is strictly related to the net donor ability of the ligand, while in the carbonyl compounds of gold(I) this correlation is essentially absent and the data are more scattered. A generalization of CD analysis allows us to describe quantitatively the ligand−metal bond in terms of Dewar−Chatt−Duncanson (DCD) bonding components[54,55] of donation and back-donation. A detailed comparative analysis of these bonding components in $[(L)Au(CO)]^{+/0}$ reveals unique information about the *trans* effect of the ligand mediated by the gold. Finally, we shall study how the CO stretching frequency in these gold complexes actually correlates with the DCD bonding components.

METHODS AND COMPUTATIONAL DETAILS

Equilibrium geometries, harmonic frequencies, and electron densities were calculated by using density functional theory (DFT) with the BLYP GGA functional[56,57] as implemented in the ADF package,[58−60] in combination with a fine integration parameter (with a numerical integration parameter set to 6). A triple-ζ basis set with two polarization functions on all atoms (TZ2P) was used. Relativistic effects were included with the zero-order regular approximation (ZORA) Hamiltonian,[61−63] with a small frozen core in computing equilibrium geometries and interaction energies, and with a large frozen core for the computation of electron densities.

In the case of **H_Au** and **CN_Au**, the vibrational coupling between the ligand and the CO has been eliminated through an isotopic substitution (^3H in the case of **H_Au** and ^{28}N for **CN_Au**). For nickel complexes, no ligand showed remarkable vibrational couplings.[12] In order to give an accurate and objective estimation of the charge transfer (CT) between the metal and the ligand, we applied the analysis of the charge displacement function (CDF). It relies on the integration along a given direction z (eq 1) of the difference of electronic density $[\Delta\rho(x,y,z)]$ between the complex and its non-interacting fragments placed in the same positions they occupy in the complex (in our case L and $[Au(CO)]^+/[Ni(CO)_3]$ for Au/Ni complexes).

$$\Delta q(z) = \int_{-\infty}^{+\infty} dx \int_{-\infty}^{+\infty} dy \int_{-\infty}^{z} dz' \Delta\rho(x, y, z') \quad (1)$$

The function $\Delta q(z)$ defines, at each point of z along a chosen axis, the amount of electronic charge that, upon formation of the bond (L−M), has moved across a plane perpendicular to the axis through the point. The CDFs give us a quantitative picture of the actual charge redistribution due to the coordination bond. In order to quantify the electron-donating ability of a ligand to the metal fragment, and in particular for the purpose of discussing the CT between L and metal carbonyl moieties, it is useful to fix a plausible boundary separating the fragments in the complexes. We choose the isodensity value representing the point on the z axis at which equal-valued isodensity surfaces of the isolated fragments are tangent.[49] The value of $\Delta q(z)$ at the isodensity gives a measure of the ligand-to-metal CT, which is an indication of the donor power of L. The convergence of CDF has been verified with respect to the basis set and the exchange-correlation functional employed, including also the relativistic effects at the full four-component level (Figures S3 and S4, in the Supporting Information).[64] As previously demonstrated for suitable symmetric complexes and fragments, $\Delta\rho$ and, consequently, $\Delta q(z)$ have been decomposed into additive symmetry components, which can be readily identified with the Dewar−Chatt−Duncanson components of the L-metal bond (Supporting Information).[49,51,65] This represented a key tool for the interpretation and rationalization of our findings.

RESULTS AND DISCUSSION

Nickel Complexes. All the nickel complexes show a ν_{CO} value smaller (red-shifted) than that of free CO (Table 1). Consistent with this, all the C−O distances are longer than that of free CO, indicating a weakened bond. However, the C−O

dx.doi.org/10.1021/ic501574e | Inorg. Chem. 2014, 53, 9907−9916

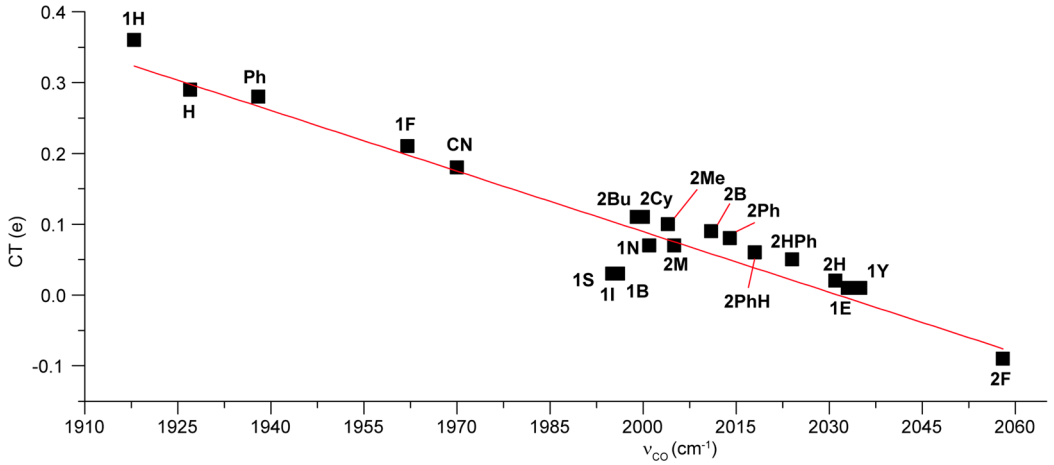

Figure 1. Correlation between CT and ν_{CO} for complexes **L_Ni**. The solid red line represents the linear best fit, whose equation is CT = $-(2.8 \pm 0.2) \times 10^{-3}$ ν_{CO} + (5.8 ± 0.4) (r^2 = 0.8955).

bond length presents a maximum variation of only 2.5 pm, whereas ν_{CO} appears more wide-ranging, with a variation up to 140 cm^{-1}. The interaction energy between the two fragments, L and [Ni(CO)$_3$], ranges from −76 to −12 kcal/mol for **1H_Ni** and **1Y_Ni**, respectively (Table S1, Supporting Information).

The net CT has been evaluated as the value of the CDF at the isodensity boundary (see Methods and Computational Details) and is reported in Table 1. These values give a quantitative estimate of the net electron donor ability of the ligand and, as can be seen, lie in a wide range going from 0.355 (for the methyl group, complex **1H_Ni**) to −0.09 electrons (for the PF$_3$ group, complex **2F_Ni**). The negative sign means that, in the case of **2F_Ni**, the Ni → L back-donation slightly prevails over the L → Ni donation. This is due to the combination of the π acceptor properties of the phosphine and the presence of three electron-withdrawing fluorine atoms. In all the other cases, the L → Ni donation dominates and, as expected, it is larger for anionic ligands (**1H_Ni**, **1F_Ni**, **Ph_Ni**, **H_Ni**, **CN_Ni**) than for neutral ones. For phosphine ligands, the trend of CT is as expected: if the phosphorus bears aliphatic substituents, the donor power is larger than in the case of aromatic ones. In fact, the trend of CT values is **2Ph_Ni** < **2Me_Ni** < **2Cy_Ni** ≈ **2Bu_Ni**. The relative ν_{CO} values well reflect the same trend (Table 1).

The correlation between CT and ν_{CO} for complexes **L_Ni** is reported in Figure 1. It shows without ambiguity the validity of the TEP to define a spectrochemical series and to measure the net donating property of the ligands: stronger electron-donating ligands induce a larger red-shift of the IR stretching of the carbonyl groups.

Such a correlation is valid not only for the phosphines but for all the ligands considered here, both neutral and anionic, with different atoms directly coordinated to the nickel (phosphorus, carbon, hydrogen) and different hybridizations (sp^3, sp^2, ...). Even *dihapto* ligands as ethyne and ethene fit well in the general trend. It is remarkable that the complexes bearing H$^-$ and PF$_3$ ligands (**1H_Ni** and **2F_Ni**) fit well into the correlation, despite the former being expected to be a merely σ-donor ligand while the latter has a significant π-acceptor capability. This is a clear indication that nickel in [(L)Ni(CO)$_3$]$^{0/-}$ complexes efficiently redistributes the electronic density received from a ligand to the CO moieties, regardless of the nature of the ligand−metal interaction. We shall return later on this interesting point.

The maximum deviation from the correlation is for the two sterically voluminous carbene ligands **1I** and **1S**, whereas **1N** fits quite well in the correlation. Due to steric hindrance the $C_{carbene}$−Ni−$C_{carbonyl}$ angle is different in complexes **1N_Ni**, **1I_Ni**, and **1S_Ni**, being 107.5°, 110.7°, and 111.2°, respectively. With the aim to verify whether and how much such differences (few degrees) affect the properties of the (NHC)−Au bond, we constrained the $C_{carbene}$−Ni−$C_{carbonyl}$ angle for **1N_Ni** at 110.7°, the value assumed in **1I_Ni.** The resulting geometry is referred to as **1N′_Ni** in Table 1. The corresponding values of CT and ν_{CO} are 0.06 e and 1999 cm^{-1}, respectively, which are now in line with the values of **1I_Ni**. This demonstrates that the value of the $C_{carbene}$−Ni−$C_{carbonyl}$ angle has a marked effect on both CT and ν_{CO}. In other words, if this angle is influenced by steric effects, as in the case of **1I_Ni** and **1S_Ni**, the correlation between CT and ν_{CO} deteriorates. If the ligand **1I** and **1S** are not considered in the fitting, the quality of the latter improves significantly, with the *r*-square value increasing to 0.9716 (from 0.8955).

Gold Complexes. The gold carbonyl compounds are termed "nonclassical" because these compounds present a CO stretching frequency which is higher than that of free CO. Many authors considered such "nonclassicity" as a proof of the fact that the gold(I) fragments do not give a significant back-donation.[66,67] But both theoretical and experimental studies now recognize that a back-donation component is present and indeed represents a highly tunable component of the bond in these gold complexes,[68] with important effects in catalysis.[32,33] Frenking and co-workers showed that the polarization of the C−O bond is the main cause for the large blue shift of the CO stretching frequency.[69,70]

In Table 2 we report the results for all the Au(I) complexes considered here. We find that gold complexes bearing neutral ligands, such as phosphines and carbenes, induce a blue-shift of ν_{CO}. This fact is in agreement with experimental data on the few cationic gold carbonyl complexes experimentally characterized.[40−42]

The anionic ligands, such as, for instance, methyl (**1H_Au**) or cyanide (**CN_Au**), show a ν_{CO} that is slightly smaller than that of free CO (Table 2), in contrast with the experimental data available from the literature. Indeed, most of the neutral gold carbonyls experimentally studied have a CO stretching frequency larger (L = CF$_3$, Cl, or Br)[35−37,43] or very close (L = HB(3,5-(CF$_3$)$_2$Pz)$_3$))[38] to that of the free carbon monoxide.

dx.doi.org/10.1021/ic501574e | *Inorg. Chem.* 2014, 53, 9907−9916

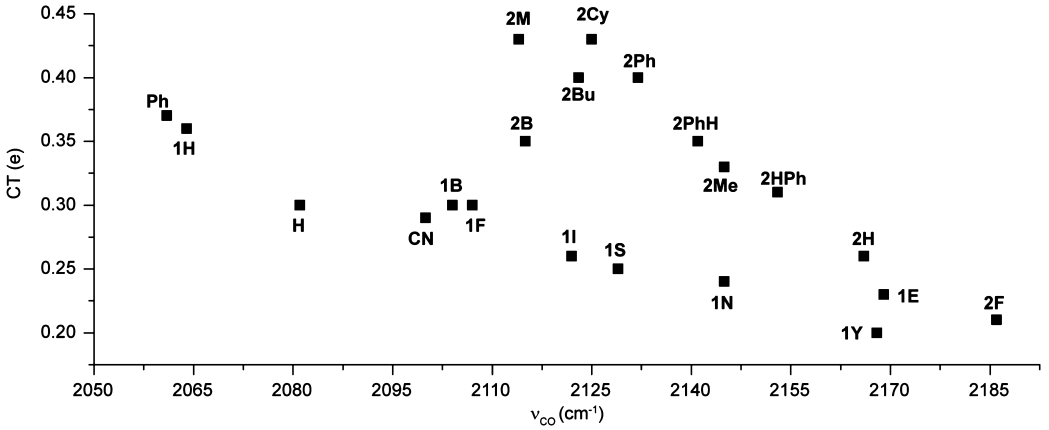

Figure 2. Trends of CT and ν_{CO} for complexes **L_Au**.

However, Dias and co-workers demonstrated that, in some of these cases, the CO frequency is blue-shifted by the presence of multimetallic adducts present under the experimental conditions.[42] Here, therefore, the CO stretching frequency cannot be reliably put in relation with the electronic property of the ligand L.

The analysis of Table 2 shows that the ligand effect in these complexes (**L_Au**) is significant and comparable with our findings for the nickel series. The C−O frequency presents a spread of about 125 cm^{-1} along the gold series, ranging from 2061 cm^{-1} in **Ph_Au** (neutral complex) to 2186 cm^{-1} in **2F_Au** (charged complex).

The CT values of Table 2 are always positive, indicating that in all cases there is a net ligand-to-metal CT, and the back-donation never prevails on the donation component of the bond. This is related to the strong Lewis acidity of the charged $[Au(CO)]^+$ fragment, which is higher than that of the neutral fragment $[Ni(CO)_3]$. As an example, the PPh_3 ligand gives a CT of 0.40 and 0.08 e in the case of **2Ph_Au** and **2Ph_Ni**, respectively. The enhanced Lewis acidity of $[Au(CO)]^+$ is also consistent with the value of the interaction energy, which, for example, is 102 kcal/mol between **2Ph** and $[Au(CO)]^+$, and 23 kcal/mol between **2Ph** and $[Ni(CO)_3]$. In general, we see that the interaction energies between L and $[Au(CO)]^+$ are typically four/five times larger than those in the corresponding complexes of nickel (Table S2, Supporting Information).

A surprising and unexpected result of our analysis is that the electronic donor power of the phosphine ligands, when coordinated to the gold atom, is generally larger than that of the NHC ligands. For instance, trimethylphosphine donates 0.33 e (complex **2Me_Au**), whereas the prototypical NHC carbene donates 0.24 e (complex **1N_Au**). Actually, the phosphines show CT values that are systematically larger than those of other ligands. As we said earlier, this result is not without precedent[24] but contrasts with what happens in nickel complexes, where **2Me_Ni** and **1N_Ni** show similar values of CT: 0.09 and 0.07 e, respectively. We surmise that the effect of the different charge of the metal carbonyl (+1 and 0 for gold and nickel, respectively) is larger on the phosphorus than on the carbon, because the former has a more polarizable lone-pair (sp^3 hybridized rather than sp^2, and larger in size) than the latter.

The plot of CT vs ν_{CO} for gold complexes appears very scattered (Figure 2). For instance, **2Me_Au** and **1N_Au**, having different CT values (0.33 and 0.24 e, respectively, Table 2), have almost the same ν_{CO} and C−O bond length, and *vice versa*, **Ph_Au** and **2PhH_Au** have a similar CT (0.37 and 0.35 e, respectively) but a $\Delta\nu_{CO}$ of about 80 cm^{-1}.

It is interesting to note that CT varies in the order **2Ph_Ni** < **2Me_Ni** < **2Bu_Ni** ≈ **2Cy_Ni** for nickel complexes and **2Me_Au** < **2Ph_Au** < **2Bu_Au** < **2Cy_Au** for gold ones. Also in the series of complexes $[(L)Cr(CO)_5]$ the nucleophilicity of the ligand increases in the order PMe_3 < PPh_3 < PCy_3,[26] and in the case of the complexes $[(L)Ir(CO)_2Cl]$, $PMe(Ph)_2$ donates slightly less electronic density than PPh_3.[14] Such "inversions" show that taking the net donor power of a ligand as an intrinsic property of the ligand itself is of course just an approximation, even within the same class of ligands, since it is finely tuned also by the electronic properties of the acceptor metal fragment.

The carbene ligands also show a different behavior with the two metals. As an example, even if the Δ(CT) between the ligands **1I** and **1S** is the same in the nickel and gold series (0.01 e), the values of $\Delta(\nu_{CO})$ are 1 and 7 cm^{-1}, respectively. It would seem that the gold atom is able to amplify the differences between the two carbenes, whose electronic properties are usually considered very similar.[21,71,72] Confirming this, the gold complex bearing the carbene with an extended aromaticity in the backbone of the ring, **1B_Au**,[73] shows a ν_{CO} value of 2107 cm^{-1}, which markedly differs from those of **1I_Au** and **1S_Au** by 22 and 15 cm^{-1}, respectively. When we consider the nickel complexes, the effect of the aromaticity on the CO frequency is negligible (in **1I_Ni**, **1S_Ni** and **1B_Ni** the spread of ν_{CO} is below 1 cm^{-1}). As also demonstrated by Gusev,[71] the introduction of an extended aromatic system on the carbene backbone leads to a maximum $\Delta(\nu_{CO})$ of 3−4 cm^{-1} in the nickel complexes, and variations of ν_{CO} of the order of 20 cm^{-1} can be obtained only through deep modifications of the carbene (such as the introduction of fluorine atoms or the substitution of nitrogen atoms with other heteroatoms). Also in the series $[(NHC)IrCl(CO)_2]$, only profound modifications of the carbene structure lead to a marked variation of ν_{CO} (30 cm^{-1}, at most).[21]

In summary, Figure 2 clearly demonstrates that, for gold complexes, the relationship between the donor power of L and ν_{CO} is not as simple as in the case of nickel, and the stretching frequency of CO cannot be used to unequivocally rank the net donor abilities of the ligands. Two complexes with the same frequency can have very different donor abilities and *vice versa*.

Before concluding this section, it is worthy of note that the remarkably different behavior of the Ni and Au complex series cannot be revealed through the analysis of the CO frequency/frequency correlation, which is typically used to compare

dx.doi.org/10.1021/ic501574e | *Inorg. Chem.* 2014, 53, 9907−9916

different spectrochemical series in metal carbonyl complexes. In Figure 3 we present the frequency/frequency plot for the **L_Ni**

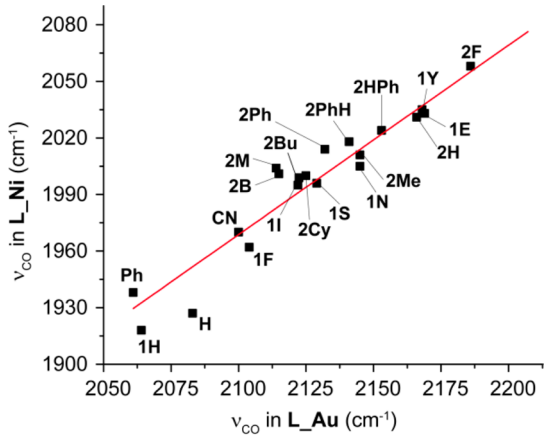

Figure 3. Linear correlation between the CO frequency in **L_Au** and **L_Ni**. The solid line represents the best fit, and its equation is ν_{CO}(**L_Ni**) = (1.04 ± 0.07)ν_{CO}(**L_Au**) − (220 ± 160)(r^2 = 0.9106).

and **L_Au** complexes. Despite the presence of some scattered data, the quality of the correlation appears acceptable (r^2 = 0.9106). Only the methyl group (**1H**), the hydride (**H**), the trimesitylphosphine (**2M**), and the JohnPhos (**2B**) are markedly out of the general trend. More importantly, no systematic differentiation between phosphines and other ligands emerges.

Looking at this frequency/frequency correlation, one would be tempted to conclude that the trend of the L−M bond properties is quite similar for gold and nickel complexes, with only some minor discrepancies. But, in light of the different effects of the L → M net donation on ν_{CO} in these complexes, which we have demonstrated above, one must conclude that this interpretation would be misleading. In other words, the interpretation underlying the TEP concept (the frequency of the carbonyl is correlated to the net donor power of L) is true for nickel complexes, but not for gold ones. Moreover, this inconsistency is not easily revealed by the comparison of the corresponding spectrochemical series. This may also be the case of other metals carbonyls and have general relevance.

With the aim to understand why the donor ability of a ligand correlates linearly with the CO stretching frequency in **L_Ni** complexes but presents a much more complex pattern in the **L_Au** series, in the following section we shall present a detailed theoretical investigation precisely addressing this interesting question.

DCD Components: [PH_3−Ni(CO)$_3$] vs [PH_3−Au(CO)]$^+$. In order to give a plausible explanation for the differences found between gold and nickel complexes (Figures 1 and 2), we present a detailed analysis of the electronic structures of these systems. If both the complex and its constituting fragments belong to the same symmetry point group, it is convenient to decompose $\Delta\rho$ into contributions from different irreducible representations.

As a case study, we consider the ligand PH_3 (**2H**) and analyze its bonding mode with the metal in **2H_Ni** and **2H_Au** complexes. Both complexes present C_{3v} symmetry with the symmetry axis passing through phosphorus and the metal. Hence, $\Delta\rho$ can be decomposed into three contributions, related to the A_1, E_1 and E_2 irreducible representations.

For the **2H_Ni** complex, the A_1 contribution involves a charge depletion on the ligand and a charge accumulation between the phosphorus and nickel that correlates with orbitals possessing σ symmetry, consistently with a ligand-to-metal σ donation, and a charge accumulation on the carbonyl moieties (Figure 4a). The shape of the latter resembles that of the

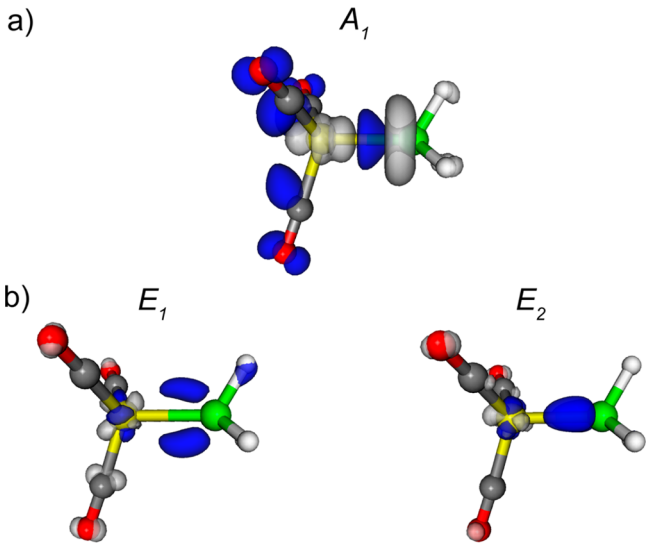

Figure 4. Three dimensional contour plots of the symmetry components of the electron density difference. (a) A_1 component. (b) E_1 and E_2 components for **2H_Ni**. Gray isosurfaces identify where the electron density is depleted, blue ones where it is accumulated. The density value at the isosurface is ±0.0022 e/(u.a.)^2.

unoccupied π^* orbitals of free CO (Figure S5, Supporting Information), the repopulation of which weakens the CO bond and decreases its stretching frequency.

On the other hand, the E_1 and E_2 contributions involve a charge accumulation on the ligand and a charge depletion on the carbonyl moieties, again with π symmetry, relatable to the π metal-to-ligand back-donation (Figure 4b). Therefore, the E contributions tend to depopulate the π^* orbitals, enforce the CO bond, and increase ν_{CO}.

A quantitative analysis of the Ni−L bond (Figure S6, Supporting Information), confirms that, in all the symmetries, the electronic density goes from the ligand to the carbonyl moieties (A_1 symmetry) and *vice versa* (E_1 and E_2 symmetries).

It thus emerges that, in the nickel complex, the metal allows all the ligand contributions to communicate with the π^* orbitals of the CO. Under this light, it is not surprising that a correlation exists between ν_{CO} and the sum of donation and back-donation (Figure 1).

A different pattern is observed when we consider the **2H_Au** complex (Figure 5). The 3D isodensity plot for the electronic density difference related to the A_1 symmetry shows again a marked charge depletion (Figure 5a) at the PH_3 (even larger than for **2H_Ni**), but this is now accompanied by a significant charge accumulation at the metal center, consistently with an electron donation from the PH_3 lone-pair into the partially empty $sd(\sigma)$ orbitals of gold.

Also in this case the A_1 contribution involves a charge accumulation on the carbonyl, but here with a cylindrical pattern and mainly located at the carbon of the CO. Its shape is consistent with a repopulation of the corresponding HOMO orbital of the free CO (Figure S5, Supporting Information),

dx.doi.org/10.1021/ic501574e | Inorg. Chem. 2014, 53, 9907−9916

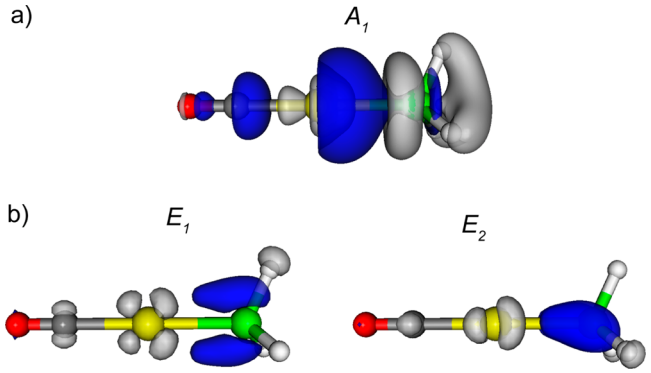

Figure 5. Three dimensional plots of symmetry-separated electron density difference. (a) A_1 component. (b) E_1 and E_2 components for **2H_Au**. Gray isosurfaces identify where the electron charge is depleted, blue ones where electron charge is accumulated. The density value at the isosurface is ±0.0022 e/(u.a.)^2.

which is mainly located on the side of the carbon facing the gold atom. Since the HOMO of the CO is a "weak bonding" orbital,[69] its repopulation is expected to cause only a small variation of the CO bond strength and, consequently, also of the CO stretching frequency (see later).

It is noteworthy that the three-dimensional plot of the A_1 contribution conveniently sums up the three-center-four-electron σ-hyperbond concept, often used to describe the Au−L ligand:[74−76] since CO and PH_3 compete for donating electronic density to the same and partially empty *sd*(σ) gold(I) orbital, the formation of the Au−L bond (with the subsequent L → Au σ donation) reduces the CO → Au σ donation (*trans* influence), as evidenced by the repopulation on the CO.

The 3D maps related to the E_1 and E_2 symmetry components of the bond (Figure 5b) show a significant charge accumulation at the PH_3 ligand region, in particular at the phosphorus site, while at the gold site there is an electron density depletion that, in shape, recalls the occupied atomic *d* orbitals of the metal. The electronic density difference on the CO reflects a change of population of the π symmetry orbitals, but, unlike the nickel complex, where the ligand induced the same electron density depletion at carbon and at oxygen sites, here an unsymmetrical pattern can be evidenced. In fact, there is a depletion on the carbon and a small accumulation at the oxygen of CO (inverse polarization, see below).

To fully understand the relationship between the charge shifts and the strength of the CO bond, it may be useful to consider the CO bonding situation in the bare $[Au(CO)]^+$ (our reference metal fragment). Here, due to the presence of Au^+, the CO bond is strongly polarized toward the carbon end and this polarization is the main cause of the large blue shift of the CO stretching frequency (2181 cm^{-1} versus 2106 cm^{-1} of the free CO) observed in $[Au(CO)]^+$.[69,70,77] The formation of a bond between an ancillary ligand L and $[Au(CO)]^+$ reduces this polarization and induces a significant reverse charge shift going from the carbon to the oxygen (inverse polarization). The consequence of the inverse polarization is a lowering of the stretching frequency with respect to the $[Au(CO)]^+$, as indeed is the case for all gold complexes considered here (see Table 2). In the system under study, **2H_Au**, the presence of the PH_3 ligand reduces the CO stretching of about 15 cm^{-1}, if compared with the bare $[Au(CO)]^+$.

According to our interpretation of the symmetry-separated electron density difference, only the components related to the metal-to-L π back-donation have an influence on the CO stretching frequency. In order to verify this and explain the scattering of data in Figure 2, a quantitative study of the ligand effect is necessary and will be presented in the next section.

DCD Components: Ligand Effect in $[(L)Au(CO)]^{+/0}$. The integration of the symmetry separated contributions of $\Delta\rho$ (CD analysis) was demonstrated to be a useful and reliable tool to quantitatively characterize the L-metal bond in terms of its DCD constituents.[49,51,64] Applying this analysis to the **2H_Au** complex analyzed before, three CDFs are obtained, corresponding to the three irreducible representations shown before and closely related to the 3D maps analyzed in the previous section. Since the curves relative to E_1 and E_2 are completely overlapping, they can be summed up in only one CDF (Figure 6). The third curve is the sum of all of three components (total), and it corresponds to the total electron density difference ($\Delta\rho$).

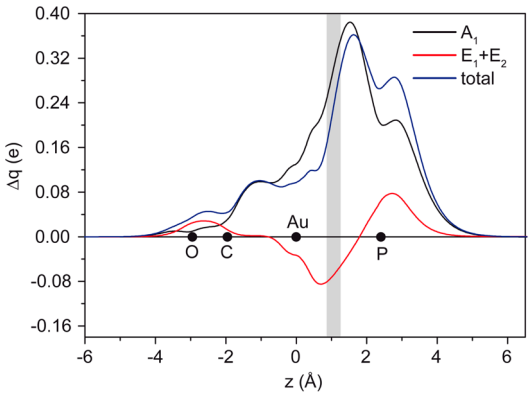

Figure 6. Symmetry-separated charge displacement curves for **2H_Au**. The black dots represent the *z* coordinate of the atoms. The vertical band identifies a suitable boundary between the metal and ligand **2H**.

In the case of **2H_Au**, the total CDF is positive throughout the whole complex (Figure 6), which is an indication of a net charge shift from L to the carbonyl. But this shift is the sum of two components. The CDF related to the *A1* symmetry is positive throughout all the molecular region, too (Figure 6), and provides a quantitative picture for the PH_3 → $[Au(CO)]^+$ σ donation component of the bond (0.32 e at the isodensity boundary). Despite the large value of CDF in the P−Au bonding region, this component dramatically decays at the carbonyl site, assuming a very small and almost constant value within the C−O bond (below 0.03 e). This pattern is consistent with the fact that the interaction between the PH_3 and the metal fragment induced a repopulation of the CO HOMO, which is located mainly on the carbon (see above).

On the contrary, the CDF curve relative to E_1 + E_2 is negative in the whole region between the metal and the phosphorus and, at the isodensity boundary, its value is −0.06 e. The negative sign indicates that the corresponding charge shift is from the gold to the ligand (π back-donation). The behavior of the CDF at the CO site is very interesting and reflects the pattern observed in the isodensity plot seen earlier. It assumes positive values in the whole region of CO, and starting from the left side of the oxygen, it increases, reaching a maximum close to the midpoint of the CO bond and then starts to decrease, crossing the zero axis in the C−Au region. The curve gives a quantitative measure of the inverse polarization induced by the presence of the ligand.

dx.doi.org/10.1021/ic501574e | *Inorg. Chem.* 2014, 53, 9907−9916

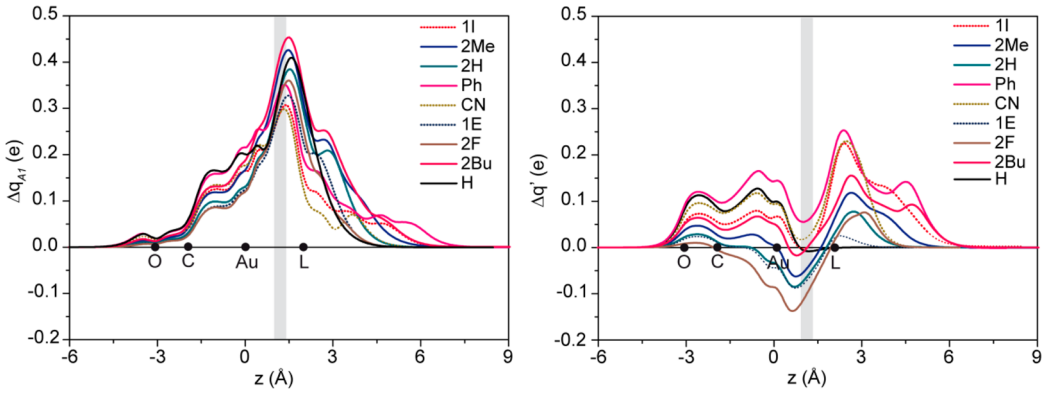

Figure 7. Symmetry-separated CD curves for all the systems studied of suitable symmetry. The black dots represent the approximate position on the z axis of the atoms in the considered complexes. The gray band represents the boundary between the two fragments. Panel on the left: $A1$ component. Panel on the right: $E_1 + E_2$ (if the molecular point group is C_{3v}) or $B_1 + B_2$ (C_{2v}).

The same method has been applied to other representative complexes, having suitable molecular symmetry and conveniently covering the whole range of possible values of ν_{CO}. In particular, we chose three complexes bearing phosphines (**2Me_Au**, **2F_Au** and **2Bu_Au**) and either neutral (**Ph_Au**, **CN_Au** and **H_Au**) or cationic (**1I_Au** and **1E_Au**) carbon-based complexes. A C_{3v} symmetry has been used for the complexes bearing phosphine ligands, while C_{2v} symmetry was used for the others. For C_{2v} symmetric complexes, $\Delta\rho$ can be decomposed into four contributions, relative to A_1, A_2, B_1, and B_2 symmetries.[49] In particular, the A_2 symmetry (which correlates with atomic d orbitals that do not participate in the bond) has not been considered, since the contribution of this component to the overall $\Delta\rho$ is negligible.[49]

The A_1 curves show a very wide range of values at the relative isodensity boundaries (gray band in Figure 7, CT_{A1} in Table 3),

Table 3. CT_{A1}, CT, and CT′ Components (in e) for Different L_Au Complexes[a]

L	CT_{A1}	CT	CT′	ν_{CO}
Ph	0.32	0.37	0.05	2061
CN	0.27	0.29	0.02	2100
H	0.31	0.300	−0.01	2081
1E	0.30	0.23	−0.08	2169
1I	0.27	0.26	−0.01	2122
2H	0.32	0.26	−0.06	2166
2Me	0.37	0.33	−0.05	2145
2Bu	0.40	0.40	0.00	2123
2F	0.31	0.21	−0.10	2186

[a]CT′ is defined as $E_1 + E_2$ for systems of C_{3v} symmetry and as $B_1 + B_2$ for systems of C_{2v} symmetry. In the last column, the corresponding values of ν_{CO} (in cm^{-1}) are reported.

but, as seen before for **2H_Au**, all of them decay in the region between the gold and the carbonyl to very small and similar values (0.02−0.04 e). Actually, all the curves almost overlap each other in this region. The picture that emerges is clear. The similarity and the small amplitude of the A_1 charge displacements observed in the CO region show that this symmetry cannot contribute significantly to the polarization of the CO bond and, anyhow, all the ligands are expected to produce the same effect on ν_{CO}.

Conversely, the electronic charge flux of π symmetry (CT′, defined as the sum of B or E components for C_{2v}- or C_{3v}-symmetric systems, respectively) assumes a wide range of values both at the isodensity boundary (CT′ goes from −0.10 to 0.05 e, Table 3) and in the CO region. The presence of the ligand induces the same trend in the two regions and considering the midpoint of the CO bond as reference, the lower is the CT′, the lower is the value that assumes the CDF of π symmetry at the CO bond.

Particularly relevant are the cases of **1I_Au** and **2Bu_Au**, which have very different values for CT_{A1}, 0.27 and 0.40 e, respectively (Table 3), and very similar values for CT′, −0.01 and 0.00 e, respectively (Table 3), due to their poor π-acceptor properties. The relative CDF π curves almost overlap in the CO region, giving the same polarization of the carbonyl and, coherently, the same ν_{CO}, 2122 and 2123 cm^{-1}, respectively.

Given all these observations, we explored the possibility, for gold complexes, of a correlation between ν_{CO} and CT′ (Figure 8). Notably, only one system, specifically **H_Au**, does not fit

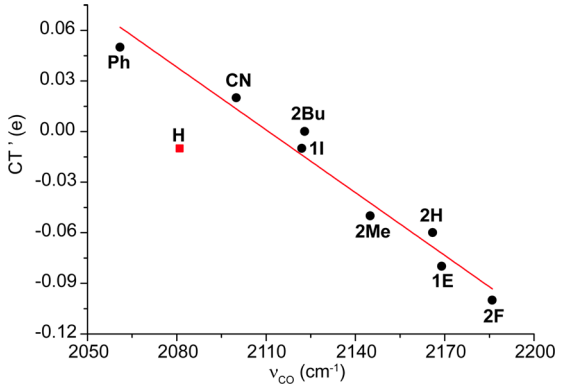

Figure 8. Linear correlation between of CT′ (the sum of $B1$ and $B2$ contributions for C_{2v} systems and the sum of $E1$ and $E2$ contributions for C_{3v} systems) and ν_{CO} for **L_Au** complexes (black squares). The solid line represents the best fit, and its equation is $CT' = -(1.26 \pm 0.09) \times 10^{-3}\nu_{CO} + (2.6 \pm 0.2)$ ($r^2 = 0.9650$). The complex **H_Au** (red circle) has been excluded from the fitting (see text for details).

well in the correlation, as if the CO polarization would be affected by an additional contribution. Such a contribution can likely be related to the electrostatic effect of the hydride ligand, which is expected to be the strongest one among the considered ligands. In fact, beyond the negative charge on L, the Au−H distance is particularly short and certainly significantly reduces the effective charge at the gold site

dx.doi.org/10.1021/ic501574e | Inorg. Chem. 2014, 53, 9907−9916

contributing to the inverse polarization. As a confirmation, **H_Au** shows a CT′ close to zero, −0.01 e (the hydride cannot accept back-donation), but the CDF at the CO site is significantly larger than those of **1I_Au** and **2Bu_Au**, for which the CT′ is close to zero, too. On the other hand, other anionic ligands fit well in the correlation (Figure 8) and the electrostatic effect seems to be less relevant. Probably it is because the negative charge they host is, on average, farther from the metal than in the case of **H_Au**.

Excluding **H_Au** from the correlation, all other ligands can be described with only one good correlation (r^2 = 0.9650), without the complex pattern present in Figure 2. This unexpected result explains most of the previous oddities: the A_1 component of the CD curve, related to the L → Au σ donation, is the most important in determining the amount of net charge transferred to the metallic fragment, but it has a negligible role in influencing ν_{CO}. On the other hand, the π component of the bond has a marked and selective effect on the polarization of the CO bond and on ν_{CO}. Among others, the case of couple of complexes **1I**/**2Bu** is eye-catching. Despite the significant difference in net CT to $[Au(CO)]^+$ (Figure 2), these systems present a very similar stretching frequency. Now, it is clear that this is because of their almost identical π components of the L−Au bond. Actually, all the difference between these two ligands relies on the σ donation component A_1 component, which is markedly different (0.27 and 0.40 e, respectively) but it does not affect the observable.

Our findings have an additional and interesting implication: it seems that the Au → L back-donation could be estimated simply from the IR spectrum (experimental or computed) of the $[(L)Au(CO)]^+$ complex. Considering the difficulties generally present in the experimental disentanglement of Dewar−Chatt−Duncanson components,[51] this result is particularly promising and deserves to be explored in detail in the near future.

CONCLUSIONS

In conclusion, our study fully confirmed, once again, the hypothesis underlying the Tolman electronic parameter, demonstrating that the net donor power of the ligand in the complex $[(L)Ni(CO)_3]^{-/0}$, evaluated through the Charge Displacement analysis of the Ni−L bond, well correlates with the A_1 stretching frequency of the CO moieties, irrespectively of the nature of the ligand. The decomposition of either the electronic density change or the CDF curves in contributions with different symmetry led to the conclusion that both σ donation and π back-donation components are effectively transmitted to the π^* orbitals of the CO moieties. For this reason, the CO stretching frequency depends on the net L → Ni donation and the donation/back-donation components cannot be disentangled in TEP. But since CT depends also on the L−Ni−CO angle, if such an angle is influenced by the steric hindrance of L, as it happens for bulky carbene ligands, the correlation is worse, as the TEP is influenced by both steric and electronic properties of the ligand.

The same study conducted for linear gold complexes $[(L)Au(CO)]^{+/0}$ led to a very different conclusion, and the correlation between the net CT and ν_{CO} appears more complex. In this case, an accurate analysis of different symmetry constituents of the DCD bonding component reveals that the A_1 component of the Au−L bond, responsible for the L → Au σ donation, is very important in determining the net CT, but it influences mainly the population of the HOMO of the carbonyl, which is known to be not important for the ν_{CO}. Moreover, such repopulation seems constant with all the ligands analyzed here. On the other hand, the π electronic flux, which is an estimation of the π acidity/basicity of the ligand, is readily transmitted to the carbonyl, polarizing the CO bond and actually determining the ligand effect on ν_{CO}. The electrostatic factor influences the CO, too, but its effect seems relevant only in the case of the hydride ligand.

For this reason, the Au-to-L π component of the bond could be, in principle, experimentally accessible just by a series of IR data for different ligands. Given the scarceness of reliable experimental data on $[(L)Au(CO)]^+$, with L possessing the appropriate symmetry and a large steric hindrance to prevent Au−Au interactions, at the present this study is possible only with DFT-generated ν_{CO} data.

Finally, it is methodologically important and of general interest to note that taking into account only the IR frequencies (measured or computed) of gold and nickel complexes would have led to the inaccurate conclusion that the trend of different L−M bonds is about the same in the two series. Only an in-depth theoretical analysis of the bond has been able to make the differences emerge. With this work, we demonstrated that the frequency−bond correlation can be much more complicated, especially if complexes with different geometries are compared.

Among the results of this work, we would like to stress the difference between the phosphine and carbene. If they are coordinated to the nickel, their donor properties are similar (0.07 and 0.08 e for a model carbene and the prototypical triphenylphosphine, respectively), but on the contrary, their abilities to donate electronic density to the gold are very different (0.24 and 0.40 e for the same carbene and phosphine, respectively), despite their very similar ν_{CO} values (2145 and 2132 cm^{-1}, respectively). In general, we found that phosphine ligands donate much more electronic density to the gold than carbene ones, even if only a part of this donation can be transmitted to the ligand in the *trans* position. Such a result is unconventional, even if not without precedents[24] and will be important to better rationalize the ligand effect in catalysis.

ASSOCIATED CONTENT

Supporting Information

Additional data, graphs, and DFT-optimized geometries for all the complexes studied. This material is available free of charge via the Internet at http://pubs.acs.org.

AUTHOR INFORMATION

Corresponding Authors

*E-mail: gciancaleoni@gmail.com.
*E-mail: leonardo.belpassi@cnr.it.

Present Address

§(N.S.) Institut Charles Gerhardt, Université Montpellier 2, ENSCM 5253, cc 1501, Place Eugène Bataillon, 34095 Montpellier Cedex 5, France.

Notes

The authors declare no competing financial interest.

ACKNOWLEDGMENTS

This work was supported by grants from the Ministero dell'Istruzione dell'Università e della Ricerca (MIUR) through FIRB-futuro in ricerca (RBFR1022UQ, Novel Au(I)-based molecular catalysts: from know-how to know-why, "AuCat").

REFERENCES

(1) Roberts, A. *Chem. News* **1898**, *78*, 260.
(2) Fischer, F.; Tropsch, H. *Brennst.-Chem.* **1923**, *4*, 276.
(3) Keim, W.; Roeper, M.; Loevenich, H.; et al. *Catalysis in C1 Chemistry*; Khimiya Leningradskoe Otd.: 1987.
(4) Calderazzo, F. *Angew. Chem.* **1977**, *89*, 305.
(5) Ozawa, F.; Soyama, H.; Yanagihara, H.; Aoyama, I.; Takino, H.; Izawa, K.; Yamamoto, T.; Yamamoto, A. *J. Am. Chem. Soc.* **1985**, *107*, 3235.
(6) Shen, J. K.; Gao, Y. C.; Shi, Q. Z.; Basolo, F. *Coord. Chem. Rev.* **1993**, *128*, 69.
(7) Hartley, F. R., Patai, S., Eds. *The Chemistry of Functional Groups. The Chemistry of the Metal−Carbon Bond, Vol. 1: The Structure, Preparation, Thermochemistry and Characterization of Organometallic Compounds*; John Wiley and Sons: 1982.
(8) Cotton, F. A.; Kraihanzel, C. S. *J. Am. Chem. Soc.* **1962**, *84*, 4432.
(9) Tolman, C. A. *Chem. Rev.* **1977**, *77*, 313.
(10) Crabtree, R. H. *The Organometallics Chemistry of the Transition metals*, 4th ed.; John Wiley & Sons Inc.: Hoboken, 2005.
(11) Kalescky, R.; Kraka, E.; Cremer, D. *Inorg. Chem.* **2014**, *53*, 478.
(12) Perrin, L.; Clot, E.; Eisenstein, O.; Loch, J.; Crabtree, R. H. *Inorg. Chem.* **2001**, *40*, 5806.
(13) Chianese, A. R.; Kovacevic, A.; Zeglis, B. M.; Faller, J. W.; Crabtree, R. H. *Organometallics* **2004**, *23*, 2461.
(14) Kelly Iii, R. A.; Clavier, H.; Giudice, S.; Scott, N. M.; Stevens, E. D.; Bordner, J.; Samardjiev, I.; Hoff, C. D.; Cavallo, L.; Nolan, S. P. *Organometallics* **2007**, *27*, 202.
(15) Leuthaeusser, S.; Schwarz, D.; Plenio, H. *Chem.—Eur. J.* **2007**, *13*, 7195.
(16) Tonner, R.; Frenking, G. *Organometallics* **2009**, *28*, 3901.
(17) Strohmeier, W.; Mueller, F. J. *Z. Naturforsch., B: Anorg. Chem., Org. Chem., Biochem., Biophys., Biol.* **1967**, *22*, 451.
(18) Darensbourg, D. J.; Nelson, H. H.; Hyde, C. L. *Inorg. Chem.* **1974**, *13*, 2135.
(19) Kuehl, O. *Coord. Chem. Rev.* **2005**, *249*, 693.
(20) Fey, N.; Orpen, A. G.; Harvey, J. N. *Coord. Chem. Rev.* **2009**, *253*, 704.
(21) Nelson, D. J.; Nolan, S. P. *Chem. Soc. Rev.* **2013**, *42*, 6723.
(22) Roodt, A.; Otto, S.; Steyl, G. *Coord. Chem. Rev.* **2003**, *245*, 121.
(23) Gusev, D. G. *Organometallics* **2009**, *28*, 763.
(24) Getty, K.; Delgado-Jaime, M. U.; Kennepohl, P. *J. Am. Chem. Soc.* **2007**, *129*, 15774.
(25) Huang, J.; Schanz, H.-J.; Stevens, E. D.; Nolan, S. P. *Organometallics* **1999**, *18*, 2370.
(26) Lee, M.-T.; Hu, C.-H. *Organometallics* **2004**, *23*, 976.
(27) These correlations are reported for easy reference in the Supporting Information (Figure S1 and S2).
(28) Hashmi, A. S. K. *Angew. Chem., Int. Ed.* **2010**, *49*, 5232.
(29) Arumugam, K.; Varghese, B.; Brantley, J. N.; Konda, S. S. M.; Lynch, V. M.; Bielawski, C. W. *Eur. J. Org. Chem.* **2014**, *2014*, 493.
(30) Seidel, G.; Fürstner, A. *Angew. Chem., Int. Ed.* **2014**, *53*, 4807.
(31) Fürstner, A.; Morency, L. *Angew. Chem., Int. Ed.* **2008**, *47*, 5030.
(32) Hashmi, A. S. K. *Angew. Chem., Int. Ed.* **2008**, *47*, 6754.
(33) Echavarren, A. M. *Nat. Chem.* **2009**, *1*, 431.
(34) Marion, N.; Diez-Gonzalez, S.; de Fremont, P.; Noble, A. R.; Nolan, S. P. *Angew. Chem., Int. Ed.* **2006**, *45*, 3647.
(35) Jones, P. G. *Z. Naturforsch., B: Anorg. Chem., Org. Chem.* **1982**, *37B*, 823.
(36) Dell'Amico, D. B.; Calderazzo, F. *Gold Bull. (London)* **1997**, *30*, 21.
(37) Belli, D. A. D.; Calderazzo, F.; Robino, P.; Segre, A. *J. Chem. Soc., Dalton Trans.* **1991**, 3017.
(38) Dias, H. V. R.; Jin, W. *Inorg. Chem.* **1996**, *35*, 3687.
(39) Kuster, R.; Seppelt, K. *Z. Anorg. Allg. Chem.* **2000**, *626*, 236.
(40) Dash, C.; Kroll, P.; Yousufuddin, M.; Dias, H. V. R. *Chem. Commun.* **2011**, *47*, 4478.
(41) Dias, H. V. R.; Dash, C.; Yousufuddin, M.; Celik, M. A.; Frenking, G. *Inorg. Chem.* **2011**, *50*, 4253.
(42) Celik, M. A.; Dash, C.; Adiraju, V. A. K.; Dias, A.; Yousufuddin, M.; Frenking, G.; Dias, H. V. R. *Inorg. Chem.* **2013**, *52*, 729.
(43) Martinez-Salvador, S.; Fornies, J.; Martin, A.; Menjon, B. *Angew. Chem., Int. Ed.* **2011**, *50*, 6571.
(44) Xu, Q.; Imamura, Y.; Fujiwara, M.; Souma, Y. *J. Org. Chem.* **1997**, *62*, 1594.
(45) Liang, B.; Andrews, L. *J. Phys. Chem. A* **2000**, *104*, 9156.
(46) Pyykkö, P.; Zhao, Y. *Angew. Chem., Int. Ed.* **1991**, *30*, 604.
(47) Schmidbaur, H. *Chem. Soc. Rev.* **1995**, *24*, 391.
(48) Belpassi, L.; Infante, I.; Tarantelli, F.; Visscher, L. *J. Am. Chem. Soc.* **2008**, *130*, 1048.
(49) Salvi, N.; Belpassi, L.; Tarantelli, F. *Chem.—Eur. J.* **2010**, *16*, 7231.
(50) Cappelletti, D.; Ronca, E.; Belpassi, L.; Tarantelli, F.; Pirani, F. *Acc. Chem. Res.* **2012**, *45*, 1571.
(51) Bistoni, G.; Belpassi, L.; Tarantelli, F. *Angew. Chem., Int. Ed.* **2013**, *52*, 11599.
(52) Ronca, E.; Pastore, M.; Belpassi, L.; De Angelis, F.; Angeli, C.; Cimiraglia, R.; Tarantelli, F. *J. Chem. Phys.* **2014**, *140*, No. 054110.
(53) Surry, D. S.; Buchwald, S. L. *Angew. Chem., Int. Ed.* **2008**, *47*, 6338.
(54) Lappert, M. F. *J. Organomet. Chem.* **2003**, *665*, 258.
(55) Chatt, J.; Duncanson, L. A. *J. Chem. Soc.* **1953**, 2939.
(56) Becke, A. D. *Phys. Rev. A: Gen. Phys.* **1988**, *38*, 3098.
(57) Lee, C.; Yang, W.; Parr, R. G. *Phys. Rev. B: Condens. Matter* **1988**, *37*, 785.
(58) ADF User's Guide, Release 2012.1; SCM, Theoretical Chemistry, Vrije Universiteit: Amsterdam, 2008, http://www.scm.com.
(59) Guerra, C. F.; Snijders, J. G.; Te, V. G.; Baerends, E. J. *Theor. Chem. Acc.* **1998**, *99*, 391.
(60) Te, V. G.; Bickelhaupt, F. M.; Baerends, E. J.; Fonseca, G. C.; Van, G. S. J. A.; Snijders, J. G.; Ziegler, T. *J. Comput. Chem.* **2001**, *22*, 931.
(61) van, L. E.; Baerends, E. J.; Snijders, J. G. *J. Chem. Phys.* **1993**, *99*, 4597.
(62) van, L. E.; Baerends, E. J.; Snijders, J. G. *J. Chem. Phys.* **1994**, *101*, 9783.
(63) van, L. E.; Ehlers, A.; Baerends, E.-J. *J. Chem. Phys.* **1999**, *110*, 8943.
(64) Belpassi, L.; Storchi, L.; Quiney, H. M.; Tarantelli, F. *Phys. Chem. Chem. Phys.* **2011**, *13*, 12368.
(65) Zuccaccia, D.; Belpassi, L.; Macchioni, A.; Tarantelli, F. *Eur. J. Inorg. Chem.* **2013**, *2013*, 4121.
(66) Gorin, D. J.; Toste, F. D. *Nature* **2007**, *446*, 395.
(67) Krossing, I. *Angew. Chem., Int. Ed.* **2011**, *50*, 11576.
(68) Alcarazo, M.; Stork, T.; Anoop, A.; Thiel, W.; Fürstner, A. *Angew. Chem., Int. Ed.* **2010**, *49*, 2542.
(69) Frenking, G.; Loschen, C.; Krapp, A.; Fau, S.; Strauss, S. H. *J. Comput. Chem.* **2007**, *28*, 117.
(70) Lupinetti, A. J.; Fau, S.; Frenking, G.; Strauss, S. H. *J. Phys. Chem. A* **1997**, *101*, 9551.
(71) Gusev, D. G. *Organometallics* **2009**, *28*, 6458.
(72) Back, O.; Henry-Ellinger, M.; Martin, C. D.; Martin, D.; Bertrand, G. *Angew. Chem., Int. Ed.* **2013**, *52*, 2939.
(73) Ciancaleoni, G.; Biasiolo, L.; Bistoni, G.; Macchioni, A.; Tarantelli, F.; Zuccaccia, D.; Belpassi, L. *Organometallics* **2013**, *32*, 4444.
(74) Benitez, D.; Shapiro, N. D.; Tkatchouk, E.; Wang, Y. M.; Goddard, W. A.; Toste, F. D. *Nat. Chem.* **2009**, *1*, 482.
(75) Landis, C. R.; Weinhold, F. *J. Comput. Chem.* **2007**, *28*, 198.
(76) Ibrahim, N.; Vilhelmsen, M. H.; Pernpointner, M.; Rominger, F.; Hashmi, A. S. K. *Organometallics* **2013**, *32*, 2576.
(77) Goldman, A. S.; Krogh-Jespersen, K. *J. Am. Chem. Soc.* **1996**, *118*, 12159.